

# INTERFACE SHAPE AND SUPERELEVATION IN CURVED STRATIFIED FLOWS

BY L. N. CHIKWENDU \*

## Introduction

The existence of transverse pressure gradient is an inherent characteristic of all rotational and irrotational curved flows. This pressure gradient is made manifest by an inward free surface inclination for the case of curved open channel flows involving homogeneous fluids. From Euler's equation, given by:

$$(\partial P / \partial r) = \rho V^2 / r \quad (1)$$

where  $\partial P / \partial r$  is the radial pressure gradient and  $V$  is the local velocity at a radius  $r$ , it is possible to carry out a one-dimensional analysis for the free surface superlevation by assuming that a constant mean velocity  $V_0$  acts at the centre-line radius  $r_c$  of the bend. Integration of equation (1) over the channel width yields:

$$h_o - h_i = \Delta h = (V_0^2 / g) (b / r_c) \quad (2)$$

where  $h_o$  and  $h_i$  are the water levels at the outer and inner walls respectively, and  $b$  is the width of the channel.

The experiments carried out by a number of early workers have, however, established that at a short distance from the beginning of a bend both the velocity and pressure distributions in a sub-critical homogeneous fluid flow are well described by a free vortex. Shukry (1950), for instance, has compared the one-dimensional theory given in equation (2) with results obtained experimentally and noted that the actual transverse free surface profile was nearly represented by the hyperbolic

shape of a free vortex, whereas equation (2) gives a linear profile. Also, the observed amount of transverse superlevation was found by Shukry to be better approximated by a modified free vortex formula.

For a sufficiently long bend, the transverse surface slope and the associated secondary circulations bring about a vertical and radial redistribution of stream velocity by mechanism of momentum transport. These changes in velocity pattern give rise to the gradual shift of high velocity filament from the inner wall to the outer wall, with the ultimate suppression of free vortex and a development of forced vortex pattern. In more recent work, Ippen and Drinker (1962) have shown that provided the mean radius to width ratio of a given channel bend is greater than unity, the magnitude of transverse superlevation in sub-critical homogeneous fluid flow is fairly approximated by the one-dimensional theory of equation (2) irrespective of the form of lateral distribution of axial velocity component. The shape of the transverse free surface profile is, however, dependent on the radial distribution of axial velocity component.

As no work seems to have been reported on the transverse interface shape and superlevation in curved stratified flows, it is intended herein to present the results of a series of laboratory tests carried out while the writer was on leave at the College of Science & Technology, University of Manchester. In these tests, two forms of stratified flow were considered, (a) the « underflow » wherein a layer of fluid flowed beneath a fairly stationary layer of slightly less dense fluid; and (b) the « overflow-with-underflow » in which the upper fluid and the lower denser fluid layers both flowed in turbulent motion

\* Lecturer in Civil Engineering, University of Nigeria Nsukka (Nigeria).

in the same general direction. The density differences between the upper and the lower fluid layers covered in these tests are within the range found in thermally stratified rivers.

---

**Notation**

---

The following symbols have been adopted for use in this paper:

- $b$  : width of curved channel;
- $\mathcal{F}_\Delta$  : densimetric Froude number  
 $= V_0/\sqrt{[\Delta\rho/\rho]gh}$ ;
- $H$  : total depth of the upper and lower layers in an underflow;
- $h$  : depth of the flowing layer(s);
- $h_i, h_o$  : interface height at the inner and outer walls respectively;
- $\Delta h$  : total transverse superelevation ( $h_o - h_i$ );
- $P_1, P_2$  : mean pressures experienced by the upper and lower layer at a given radius respectively;
- $P_2^1$  : mean pressure in the lower layer due to its own depth at a given radius;
- $\Delta P_2^1$  : pressure difference in the lower layer between the outer and the inner walls;
- $Q$  : total discharge of the flowing layer(s);
- $q_r$  : percentage ratio of the discharge of the upper layer to that of the lower layer in an overflow-with-underflow;
- $\mathcal{R}$  : Reynolds number  $= V_0 h/\nu$ ;
- $r$  : radial distance to a point in curve;
- $r_c$  : centreline radius of bend;
- $V$  : local axial velocity at a bend radius  $r$ ;
- $V_0$  : mean axial velocity of the flowing layer(s);
- $V_1, V_2$  : mean velocities of the upper and lower layers respectively;
- $Z$  : vertical distance measured from the channel bed;
- $\rho$  : mass density of lower fluid layer;
- $\Delta\rho$  : density difference between the lower and upper fluid layers;
- $\nu$  : kinematic viscosity of fluid;
- $\lambda$  : ratio of channel width to centreline radius of bend  $= b/r_c$ .

---

**Experimental equipment and method**

---

Hot water and cold water were used to simulate the upper and lower layers respectively.

The experimental channel was made up of a stilling basin which was flared on the bottom and sides to give smooth entry to the flume. The basin was fed through a 2-inch pipe which discharged cold water vertically downward onto the bed at the centre of the end wall. Surface waves within the basin were suppressed by a floating wooden board placed on the water surface.

The stilling basin was joined onto a 135° curved unit by a 40-inch straight approach length. The centreline radius of curvature of the curved unit was 60 inches. The width and height of the rectan-

gular channel section were 10 ins. and 9 3/4 ins. respectively. The downstream end of the curved unit had a 40-inch straight exit length which terminated in a small outlet tank. The tank incorporated a tilting weir for adjusting water level, and a vertical recess for inserting a sluice gate used in controlling the pool of the upper layer during the « underflow » tests. Schematic diagrams of the arrangements for flow control are shown in figs 1 and 2. Because of the transparency of the perspex material used for the bottom and walls of the entire channel, visual observations were made possible. The channel rested on supports which were levelled to keep the bed horizontal throughout the tests.

The outlet end of a thermostatic mixing valve was connected to a rubber hose which delivered hot water into the flume through a manifold-pipe distributor. The hot water distributor spanned the width of the stilling basin and rested on the floating board in the basin just above the cold water level. Discharge of hot and cold water were recorded by previously calibrated elbow meter and orifice plate respectively. Precise and rapid measurements of temperature readings were achieved by the use of a commercial direct-reading multipoint thermistor instrument which incorporated twelve sensing probes and had a scale graduated in degree Fahrenheit. Each miniature semi-conductor sensing element of the instrument was mounted at the last one-quarter inch length of stainless tubing, 1 ft. long and 0.0625 inch outside diameter. From the temperature readings it was possible to determine the densities and locate interfaces. Velocity measurements were not made, as the local velocities were generally too small to be recorded with the available instrument. The free surface levels were measured by means of micrometer point gauges.

For the underflow tests, a sluice gate was inserted in position to give an opening of 1 1/2 inch at the end of the channel while the tilting weir was raised so as to retain a pool of hot water in the entire channel (see Fig. 1). The desired amount of cold water discharge was then slowly turned on until a quasi-steady state was attained whereby the cold layer flowed underneath the layer of warm water, through the sluice gate and over the weir before discharging to waste. The total depth of hot and cold water was kept constant at 6.5 ins. throughout the tests.

In the case of overflow-with-underflow tests, (see Fig. 2) the general procedure adopted in superposing the two streams consisted of first turning on the required amount of cold water, allowing it to stabilise before turning on the hot water. A fair degree of initial mixing was eliminated as the hot water jets from the distributor fell on the floating wooden board within the stilling basin. The two streams then flowed along the channel after being controlled in the straight approach length by a series of parallel blades. The tilting weir was used to achieve variations in total depth of flow.

In all the tests, the temperature distribution and the interface form were determined by vertical temperature traverses taken at the central section of the bend; except for a few tests in which further measurements were taken along the bend. The temperature readings at a given section were recorded with five probes spaced radially at 2 1/2 inches

apart, and held by horizontal rigid perspex bar. The perspex bar was in turn carried by a bent iron rod which was fixed to a micrometer screw gauge, thereby allowing simultaneous lowering or raising of all five probes to any desired depth. Surface and bed temperature readings were taken at 0.25 ins. from the free surface and bed respectively. Intermediate readings were taken at 0.5 ins. vertical intervals except near the interfacial zone where this was reduced to 0.25 inch intervals.

The range of various variables covered in the tests is summarised in Table 1.

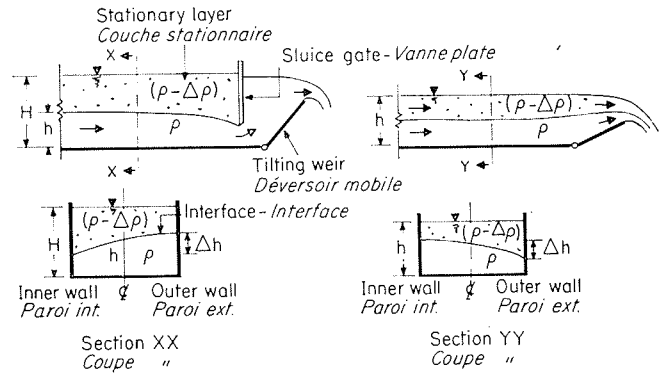
**Interface shape**

**Underflow :** Visual observation of the longitudinal and transverse interface profiles were made by colouring the upper layer with a suitable dye. The longitudinal interface profile was fairly uniform over the bend but became slightly depressed in the straight outlet length. Near the sluice end, where the cold water layer was compelled to flow through the 1 1/2 inch opening, the longitudinal interface slope became relatively steep showing resemblance to the "free overfall" profile in free surface flow of a homogeneous fluid. A photograph of the longitudinal profile looking from the outer wall of the underflow can be seen in Figure 3.

Across the channel width, visual observations alone showed a deeper cold water region on the outer wall of the bend than on the inner wall, thus reflecting on the transverse interface super-elevation. The experimental shapes of the interfaces at mid-bend for various values of densimetric Froude number ( $\mathcal{F}^{\Delta}$ ) are shown in Figure 4. The interface positions were obtained by plotting each temperature profile on an enlarged scale, constructing the tangent at the point of inflexion and hence determining the interface height.

As can be observed from Figure 4, there is a close similarity between all the transverse interface profiles obtained, except for slight differences which arose from the varying wall effects. Because a description of the patterns of secondary currents in curved stratified flows will be the subject of a forthcoming paper, it will be remarked in passing here that although these secondary currents are primarily responsible for the interfacial mixing of the two layers, yet they effected mixing only to a small extent and so permitted the interfaces to be located with some degree of accuracy. Entrainment of the upper layer was very small.

**Overflow-with-Underflow :** At a bend angle smaller than  $\pi/8$  the interface height near the inner wall was found to increase downstreamwards with the opposite behaviour on the outer wall. The visual transverse super-elevations in this region were also found to be large in comparison to that over the rest of the channel bend. Beyond  $\pi/8$ , however, the super-elevation appeared to be constant along the bend. These observations were confirmed by actual measurements of interface super-elevations at bend angles of  $\pi/8$ ,  $3\pi/8$  and  $5\pi/8$  respectively, from which the super-elevation at  $3\pi/8$  and  $5\pi/8$  differed only slightly whereas that at  $\pi/8$  was found to be about 50 % larger than any of the



1/ Schematic diagram of curved stratified "underflow".

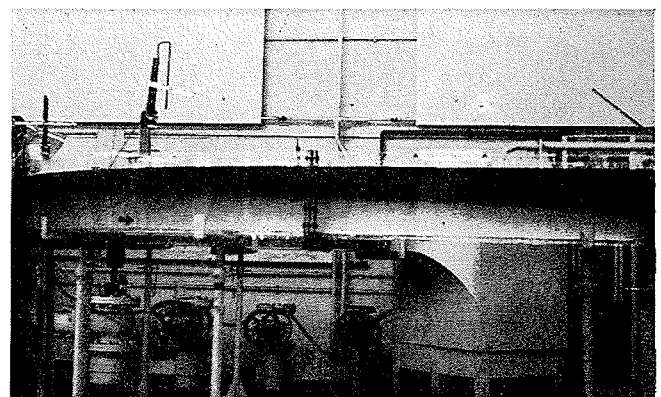
*Schéma d'un « sous-écoulement » courbe stratifié.*

2/ Schematic diagram of curved stratified "overflow-with-underflow".

*Schéma d'un écoulement mixte : « sur-écoulement avec sous-écoulement », courbe et stratifié.*

**Table 1**  
Range of tests

VARIABLE	UNDERFLOW	OVERFLOW-WITH-UNDERFLOW
Overall depth . . . . (ins)	H = 6.5	h = 2.3 to 6.3
Total discharge Q . (in <sup>3</sup> /sec)	17.03 to 52.9	32.6 to 72.0
Discharge ratio $q_r$ . . . . .	—	40 % and 80 %
Density difference ratio . . . . . ( $\Delta\rho/\rho$ )	0.45.10 <sup>-3</sup> to 0.469.10 <sup>-2</sup>	0.49.10 <sup>-3</sup> to 0.434.10 <sup>-2</sup>
Sluice opening . . . . (ins)	1.5	—
Densimetric Froude Number . ( $\mathcal{F}^{\Delta}$ )	0.38 to 0.725	0.338 to 2.42
Reynolds Number.. ( $\mathcal{R}$ )	1.1.10 <sup>3</sup> to 3.34.10 <sup>3</sup>	3.84.10 <sup>3</sup> and 4.65.10 <sup>3</sup>



3/ 135° test flume showing longitudinal interface profile in an "underflow".

*Canal d'essai courbé à 135° mettant en évidence le profil de l'interface longitudinale dans un « sous-écoulement ».*

former. In the circumstances, it would appear that the bend entry conditions influenced the interface shape and superelevation at bend angles smaller than  $\pi/8$ . This is to be expected since the flow could be thought to be then in its adjusting process.

In Figure 5 are shown some of the experimental transverse profiles of the interface for various values of densimetric Froude numbers, total depths and discharge ratios. While there seems to be a close similarity between the shapes of these interfaces, it will be observed that some difference exists when comparison is made with those found for the underflows. In particular, the direction of the interface curvature has been reversed in the overflow-with-underflow, the deepest cold water layer being now on the inner wall.

At small depths and large densimetric Froude number of the order of 2.5 or higher, the locus of the interface intersected the channel bed near the outer wall, with the cold water layer virtually exposed at the free surface on the inner wall. This behaviour of the interface in an overflow-with-underflow tended to set the upper limit of the densimetric Froude number which could be investigated in small scale laboratory experiments of this nature.

The rather peculiar interface shape of the overflow-with-underflow, in which the deepest cold water layer is found on the inner wall rather than on the outer wall, is well in accord with a simple theoretical argument which can be formulated as follows:

Consider two co-current stratified layers flowing within a curved channel of mean radius  $r_c$ , and assume that the lighter upper layer of density ( $\rho - \Delta\rho$ ) and the lower layer of density  $\rho$  move with mean velocities of  $V_1$  and  $V_2$  respectively. If the mean pressure experienced by the upper layer is  $P_1$  and that of the lower layer is  $P_2$ , then the mean pressure  $P_2^1$  of the lower layer due entirely to its own depth will be given by:

$$P_2^1 = P_2 - P_1 \quad (3)$$

where  $P_1$ ,  $P_2$  and  $P_2^1$  all vary with  $r$  only.

From Euler's equation, and by carrying one-dimensional analysis for the upper and lower layers, the following are obtained:

$$(dP_1/dr) = (\rho - \Delta\rho) (V_1^2/r_c) \quad (4)$$

and:

$$dP_2/dr = \rho V_2^2/r_c \quad (5)$$

So that:

$$dP_2^1/dr = (\rho/r_c) [V_2^2 - (1 - \Delta\rho/\rho) V_1^2] \quad (6)$$

For the order of density differences under consideration,  $(1 - \Delta\rho/\rho) \approx 1.0$ . Equation (6) is therefore reduced to the form:

$$dP_2^1/dr = (\rho/r_c) (V_2^2 - V_1^2) \quad (7)$$

On integrating equation (7) across the channel yields:

$$\Delta P_2^1 = (\rho b/r_c) (V_2 + V_1) (V_2 - V_1) \quad (8)$$

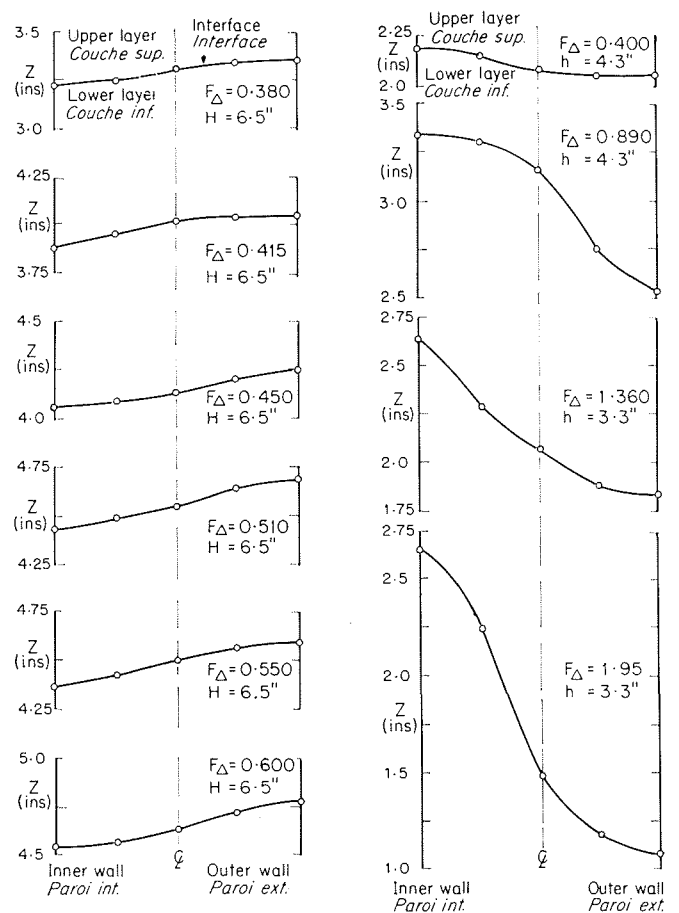
where  $b$  is the width of the channel.

In equation (8)  $\Delta P_2^1$  is the positive pressure difference in the lower layer between the outer and the inner wall. It is therefore clear from equation (8) that if  $V_2 < V_1$ , as is generally the case in stratified

overflow-with-underflow with turbulent motion in the two layers, then  $\Delta P_2^1$  will be negative and there will be larger depth of the lower layer on the inner wall than on the outer wall. When  $V_1 \rightarrow 0$ , as obtains in stratified underflow or in free surface flow of a homogeneous fluid, then  $\Delta P_2^1$  becomes positive and there will be larger depth of the lower layer on the outer wall than on the inner wall. Thus in curved stratified flows with slight density differences and in which both the upper and lower fluid layers are in turbulent motion, the interfacial shape is such that the largest depth of the lower layer will be found on the inner wall and the largest depth of the upper layer on the outer wall.

### Transverse superelevation

*Underflow:* One characteristic of stratified flows which has emerged from the present studies is the magnification of the interface transverse superelevation as compared to the corresponding free surface superelevation in a homogeneous fluid flow. From one-dimensional analysis for a homogeneous

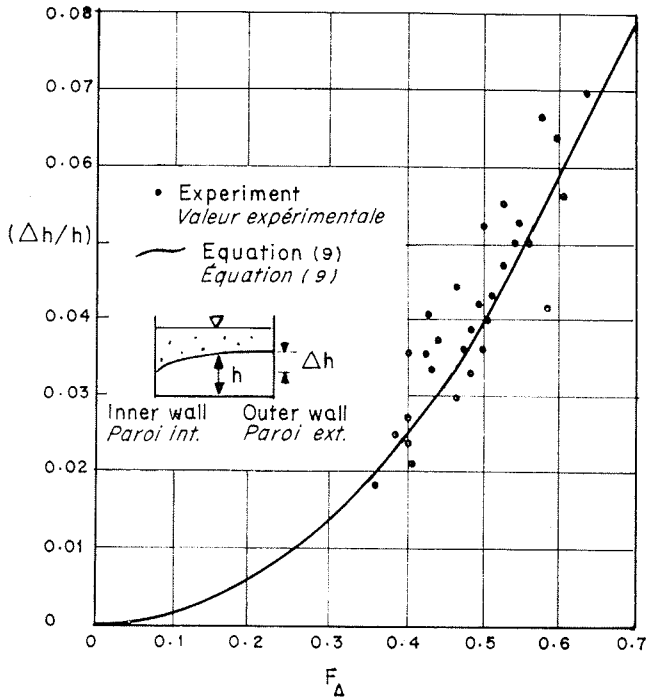


4/ Interface transverse profiles in an "underflow".

*Profils en travers de l'interface dans un « sous-écoulement ».*

5/ Interface transverse profiles in an "overflow-with-underflow".

*Profils en travers de l'interface dans un écoulement mixte : « sur-écoulement avec sous-écoulement ».*



6/ Correlation of interface superlevation in an "underflow".  
 Corrélation entre différentes surélévations de l'interface dans un « sous-écoulement ».

fluid, it has been shown that the total transverse superlevation is given by:

$$\Delta h = (V_0^2/g) (b/r_c) \quad (2)$$

whereas for a stratified underflow, similar analysis will give the interface transverse superlevation as:

$$\Delta h = [V_0^2/(\Delta\rho/\rho) g] (b/r_c)$$

or:

$$(\Delta h/h) = \lambda F_{\Delta}^2 \quad (9)$$

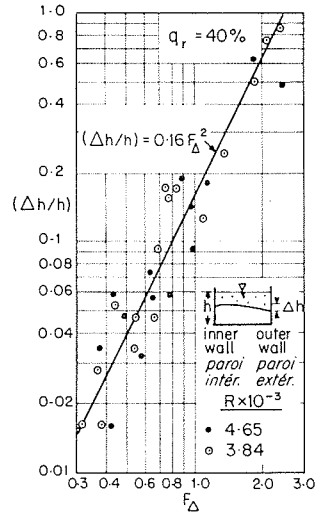
where:

$$\lambda = (b/r_c), \quad F_{\Delta}^2 = V_0^2/[\Delta\rho/\rho) gh]$$

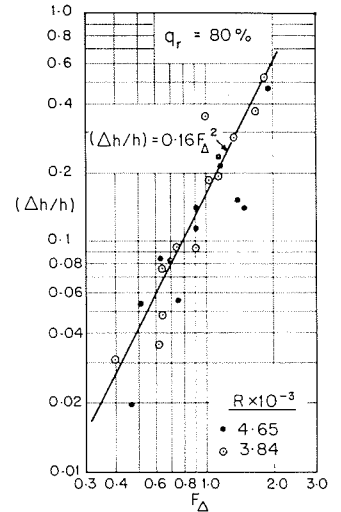
In view of the magnitude of density difference ratios ( $\Delta\rho/\rho$ ) in the stratified media under consideration, it is apparent that the interface transverse superlevation is of the order of about  $10^3$  multiplied by the free surface superlevation in a homogeneous fluid flowing under similar conditions.

A number of theoretical expressions for transverse superlevation in stratified underflows was derived by the writer by making several assumptions about the radial velocity distribution in the Euler's equation. A comparison of the results with that given by the simple one-dimensional theory of equation (9) showed largest deviation of about 8 % for the value of  $\lambda$  of one-sixth used in the present tests. It would seem, therefore, that the magnitude of the transverse superlevation in moderately curved stratified underflow is not materially influenced by the form of axial velocity distribution in the radial direction.

Figure 6 shows a plot of the experimental superelevations obtained at mid-section of the 135° bend. In the same graph the theoretical curve as given by equation (9) has been plotted for the value of  $\lambda$  of one-sixth. The experimental values of the densi-



7/ Correlation of interface superlevation in an "overflow - with - underflow" for  $q_r = 40\%$ .  
 Corrélation entre les surélévations de l'interface dans un écoulement mixte (« sur - écoulement avec sous - écoulement ») pour  $q_r = 40\%$ .



8/ Correlation of interface superlevation in an "overflow - with - underflow" for  $q_r = 80\%$ .  
 Corrélation entre les surélévations de l'interface dans un écoulement mixte (« sur - écoulement avec sous - écoulement ») pour  $q_r = 80\%$ .

metric Froude number were based on the mean velocity of the lower flowing layer and on the density differences between the upper and lower layers as measured at mid-bend section. There is a considerable scatter in experimental points which is attributable to both the error involved in the evaluation of the interface heights and to wall viscous effects. The increasing trend of the superlevation with densimetric Froude number is however easily discernible and follows closely the curve given by the one-dimensional theory.

Hence, provided that an open-channel bend has a moderate curvature ( $b/r_c < 1$ ) and is sufficiently long, the theoretical expression given in equation (9) will adequately predict the amount of transverse interface superlevation in a stratified underflow.

Attempts to measure the free surface superlevation were unsuccessful as the transverse variation in total depth was extremely small.

**Overflow-with-underflow:** Any rigorous theory for the interface superlevation in curved overflow-with underflow will require a knowledge of the distribution of axial velocities in the radial direction for both layers. Because velocity traverses were not made in the present experimental studies, it was considered that for practical convenience the results could be correlated empirically by the use of densimetric Froude number based on the mean velocity of the combined flow over the total depth, and on the density difference ratio between the two layers at mid-bend section. This approach also made it possible to check whether much error would be introduced by making use of the one-dimensional theoretical analysis of equation (9) for the interface superlevation in overflow-with-underflow.

In Figures 7 and 8 are the experimental plots of

the dimensionless transverse super-elevation in overflow-with-underflow against the densimetric Froude number based on the combined flow. Each of the two figures, which represents the discharge ratio of 40 % and 80 % respectively, contains results obtained from two different Reynolds numbers, while keeping the discharge ratio constant. Since there is no systematic scatter in the graphs, arising from the variations in Reynolds number, it can be concluded that for a given channel bend, given discharge ratio and given density difference, the magnitude of interface super-elevation is not very sensitive to variations in Reynolds number. Generally, however, the experimental points show some scatter which may again be due to the error involved in evaluating the super-elevations and on the use of densimetric Froude numbers based on the mean velocity of the two layers which paid no regard to the momentum correction factor. Nevertheless, it has been possible to fit a mean curve through the points in each graph. The agreement between the results for the two discharge ratios is fairly close, that they are well represented by the following empirical equation:

$$(\Delta h/h) = 0.16 \mathfrak{F}_\Delta^2 \quad (10)$$

It is to be noted that equation (10) is nearly the same as the one-dimensional theory of equation (9) for the given value of  $\lambda$  of one-sixth.

Thus, for a sufficiently long bend with a moderate curvature, the interface transverse super-elevation in stratified overflow-with-underflow is not materially affected by the discharge ratio and Reynolds number. The magnitude of the interface super-elevation is primarily dependent on the mean momentum of flow, density differences and width to radius ratio; and can be evaluated by applying a one-dimensional analysis to the overall flow.

---

### Summary of conclusions

---

1. In an underflow where the upper layer is relatively stationary, the interface slopes inwards with the largest depth of the lower layer on the outer wall.
2. In an overflow-with-underflow where the flows in the two layers are in turbulent motion, the interface slopes outwards with the largest depth of the lower layer on the inner wall.
3. The magnitude of the interface super-elevation is essentially dependent on the mean momentum of flow, the width to radius ratio of the channel, and the difference in specific weights of the stratified media. For channel bends of moderate curvature, the interface super-elevation is not materially influenced by the form of velocity distribution, the Reynolds number and the discharge ratio.
4. In a sufficiently long bend with moderate curvature, one-dimensional analysis for interface super-elevation can adequately predict the amount of super-elevation in stratified underflows as well as in stratified overflow-with-underflow.

---

### Acknowledgement

---

The writer would like to express his sincere gratitude to Professor J.R.D. Francis for his advice and the laboratory facilities provided.

---

### References

---

- SHUKRY (A.). — Flow around bends in an open flume. *Trans. ASCE*, Vol. 115 (1950), paper 2411, p. 751.
- IPPEN (A. T.) and DRINKER (P. A.). — Boundary shear stresses in curved trapezoidal channels. *Proc. ASCE*, Vol. 88, No. HY5 (1962), part 1, p. 143.

---

### Résumé

#### Forme et surélévation de l'interface dans les écoulements stratifiés à trajectoire courbe

par L. N. Chikwendu \*

Il s'agit, dans cette étude, de la forme et de la surélévation de l'interface dans les écoulements à stratification de densité, et suivant un parcours en courbe.

Après un résumé succinct d'études antérieures portant sur les écoulements homogènes à trajectoires courbes, on décrit l'étude expérimentale des écoulements stratifiés en deux couches. Cette étude tient compte d'écoulements stratifiés de deux natures différentes, l'un correspondant à un courant d'eau froide s'écoulant sous une couche supérieure d'eau relativement plus chaude et quasi-stationnaire et l'autre correspondant à un courant chaud, superposé sur un courant froid, tous les deux étant en régime turbulent, et s'écoulant sensiblement dans la même direction dans un canal courbe. La gamme des différences de densité étudiées se situait à l'intérieur de celle rencontrée normalement dans les rivières présentant un écoulement à stratification thermique.

On a observé les profils longitudinal et transversal de l'interface par visualisation, en teintant la couche liquide supérieure à l'aide d'un colorant approprié.

---

\* Lecturer in Civil Engineering, University of Nigeria Nsukka (Nigeria).

Dans le cas d'un courant froid s'écoulant sous une couche quasi stationnaire, on a pu constater que le profil longitudinal de l'interface du courant inférieur était assez uniforme sur l'ensemble de la courbe du canal, mais qu'il se rabattait à l'extrémité aval de ce dernier, où la couche inférieure devait s'écouler sous une vanne située dans un pertuis. L'observation visuelle a révélé que ce même courant d'eau froide était plus profond du côté de la paroi à l'extérieur de la courbe, que du côté de la paroi intérieure.

Dans le cas des deux courants superposés, on a pu constater que la forme transversale était contraire à la précédente, puisque la plus grande profondeur de la couche inférieure se situait, cette fois, du côté de la paroi intérieure. Des mesures expérimentales ont été effectuées; elles sont représentées sur les figures 4 et 5. Ces résultats ont amené à la conclusion que, pour les variables dont il a été tenu compte dans l'étude, la forme du profil transversal de l'interface n'est modifiée, ni par le nombre de Froude densimétrique, ni par le nombre de Reynolds, ni par le rapport entre la profondeur et la largeur. L'auteur présente un argument théorique, vérifiant certaines de ces observations (voir les équations 3 à 8).

Une analyse théorique unidimensionnelle a montré qu'il est possible d'exprimer la surélévation transversale  $\Delta h$  de l'interface par une relation de la forme :

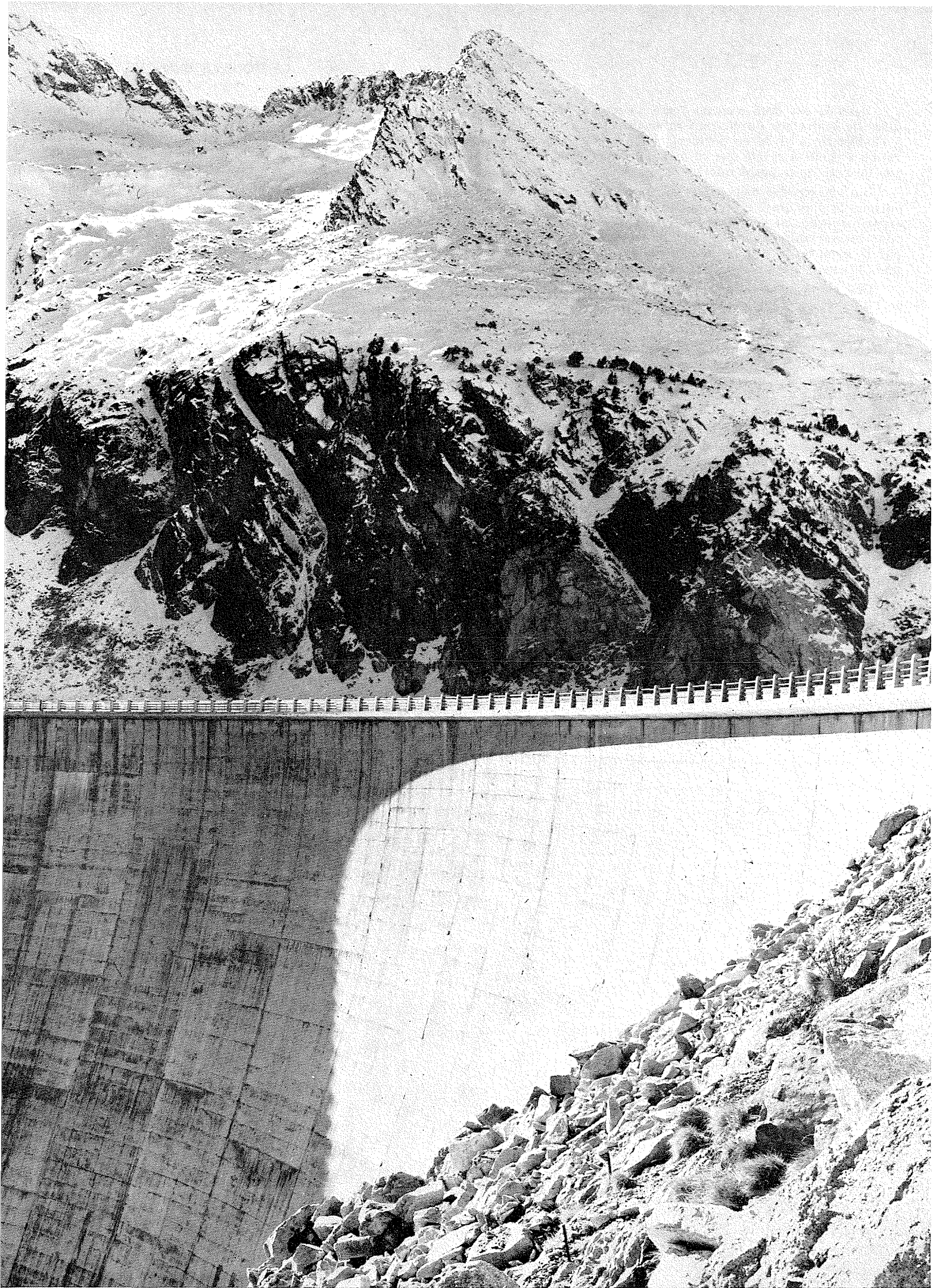
$$\Delta h/h = \lambda \mathcal{F}_\Delta^2 \quad (9)$$

dans laquelle  $h$  correspond à la hauteur d'écoulement,  $\lambda$  au rapport entre la largeur du canal et le rayon moyen, et  $\mathcal{F}_\Delta$  au nombre de Froude densimétrique, ce dernier étant donné par la relation  $\mathcal{F}_\Delta^2 = V_0^2 / (\Delta\rho/\rho \cdot gh)$ . La confrontation de l'équation (9), et d'un résultat analogue obtenu pour le cas d'un écoulement liquide homogène, indique que la valeur de la surélévation de l'interface dans un écoulement à stratification thermique, correspondrait à un multiple de l'ordre de  $10^3$  de la valeur de la surélévation ayant lieu dans un écoulement d'un liquide homogène correspondant. La figure 6 représente la surélévation mesurée dans un courant inférieur au droit de la section médiane de la courbe à  $135^\circ$ .

Cette dernière figure montre que les résultats s'accordent de près avec l'expression théorique donnée dans l'équation (9). Des résultats expérimentaux analogues, correspondant à la surélévation de l'interface, dans le cas de deux courants superposés, sont représentés sous forme graphique dans les figures 7 et 8. La relation empirique déduite, et définissant la grandeur de la surélévation de l'interface dans le cas de deux courants superposés, est de la forme :

$$\Delta h/h = 0,16 \mathcal{F}_\Delta^2 \quad (10)$$

Puisqu'il a été tenu compte, dans ces essais, d'un rapport égal à  $1/16$  entre la largeur et le rayon, on observe que les équations (9) et (10) sont identiques, et on aboutit à la conclusion que l'analyse théorique unidimensionnelle donnée dans l'équation (9) permet de déterminer d'avance les surélévations ayant lieu dans les écoulements stratifiés, quels que soient la valeur du rapport entre les débits des couches inférieure et supérieure, et le nombre de Reynolds, et quelle que soit la forme de la répartition des vitesses.



Barrage de Cap-de-Long.